
AGLA: Mitigating Object Hallucinations in Large Vision-Language Models with Assembly of Global and Local Attention

Wenbin An¹ Feng Tian¹ Sicong Leng² Jiahao Nie² Haonan Lin¹
QianYing Wang³ Guang Dai⁴ Ping Chen⁵ Shijian Lu²

¹Xi'an Jiaotong University ²Nanyang Technological University

³Lenovo Research ⁴SGIT AI Lab ⁵University of Massachusetts Boston
wenbinan@stu.xjtu.edu.cn, fengtian@mail.xjtu.edu.cn

Abstract

Despite their great success across various multimodal tasks, Large Vision-Language Models (LVLMs) are facing a prevalent problem with object hallucinations, where the generated textual responses are inconsistent with ground-truth objects in the given image. This paper investigates various LVLMs and pinpoints *attention deficiency* toward discriminative local image features as one root cause of object hallucinations. Specifically, LVLMs predominantly attend to prompt-independent global image features, while failing to capture prompt-relevant local features, consequently undermining the visual grounding capacity of LVLMs and leading to hallucinations. To this end, we propose *Assembly of Global and Local Attention (AGLA)*, a training-free and plug-and-play approach that mitigates object hallucinations by exploring an ensemble of global features for response generation and local features for visual discrimination simultaneously. Our approach exhibits an image-prompt matching scheme that captures prompt-relevant local features from images, leading to an augmented view of the input image where prompt-relevant content is reserved while irrelevant distractions are masked. With the augmented view, a calibrated decoding distribution can be derived by integrating generative global features from the original image and discriminative local features from the augmented image. Extensive experiments show that AGLA consistently mitigates object hallucinations and enhances general perception capability for LVLMs across various discriminative and generative benchmarks. Our code will be released at <https://github.com/Lackel/AGLA>.

1 Introduction

By extending Large Language Models [1, 2, 3, 4, 5] into the visual domain, Large Vision-Language Models (LVLMs) [6, 7, 8, 9, 10, 11, 12] have demonstrated impressive performance across various tasks such as image captioning [13, 14] and visual question answering [15, 16]. Despite their remarkable success, LVLMs still encounter numerous challenges that impede their applications in real-world tasks. Among these challenges, object hallucination [17, 18, 19, 20, 21, 22], where the generated textual responses by LVLMs include objects that are not present in the input image, is one prominent concern that constrains the reliability and applicability of LVLMs [23, 24].

Several studies have explored the underlying cause of object hallucinations in LVLMs, leading to different conclusions such as statistical pre-training bias [25, 26, 27], over-reliance on parametric knowledge [19, 28, 29, 30, 31], biased feature learning [22, 32, 33], etc. Despite these efforts, we conjecture that object hallucinations stem from *attention deficiency* toward images, where LVLMs predominantly attend to global image features while failing to capture prompt-relevant local features.

Is there a **building** in the image? Is there a **sky** in the image? Is there a **chair** in the image? Is there a **car** in the image?

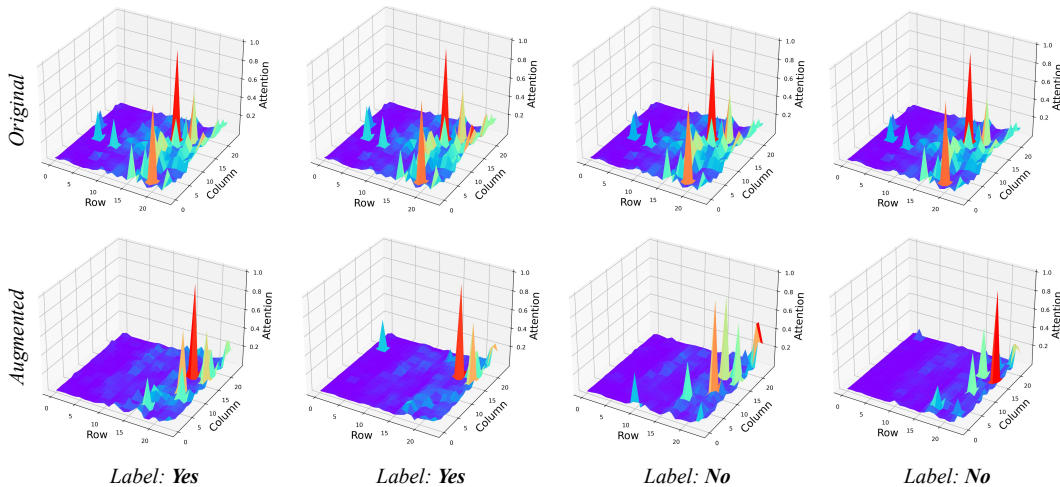


Figure 1: Self-attention weights in LVLMs with respect to image patch features when the decoder responds to different object queries (*Yes* or *No*). The **first row** shows LVLMs’ global attention toward the original input image, which is dominated by certain global image features and presents similar attention patterns consistently regardless of the queried objects. The **second row** shows LVLMs’ local attention toward augmented views of the input image, which is more prompt-dependent and captures query-relevant local features.

To verify this hypothesis, we examine self-attention weights for image patch features when LVLMs respond to queries about different objects. As the first row of Fig. 1 shows, the self-attention weights are dominated by certain global features and present similar patterns regardless of the queried objects, being present or absent in the image. This is largely attributed to *attention deficiency* toward images in LVLMs that leads to the ignorance of prompt-relevant local features that are crucial for object discrimination [34], consequently impairing LVLMs’ visual grounding ability and resulting in hallucinations. Such tendency to global features is well aligned with the recent study in [35], showing that LVLMs tend to be disturbed by prompt-independent objects through association [25, 19] (e.g., hallucinating “cars” disturbed by “road” in images). Therefore, it is crucial to incorporate prompt-dependent local attention to block out distractions and mitigate object hallucinations.

To this end, we design *Assembly of Global and Local Attention (AGLA)*, a training-free and plug-and-play approach that introduces prompt-dependent local attention to generate an augmented view of the input image to mitigate object hallucinations. Inspired by the idea of network interpretability [36, 37], we design an image-prompt matching scheme to compute the prompt-dependent attention and apply it to derive an augmented view of the original image. As illustrated in the

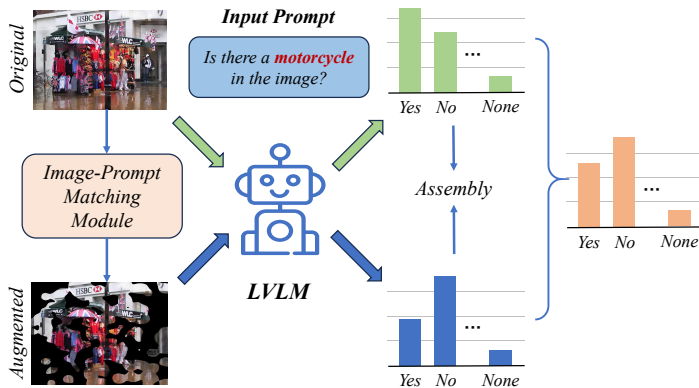


Figure 2: Decoding with *Assembly of Global and Local Attention*.

second row of Fig. 1, attention toward the augmented images is prompt-dependent, which forms a great complement to the global prompt-independent attention over the original image. Finally, as Fig. 2 shows, a calibrated decoding distribution can be derived by integrating generative global features from the original image and discriminative local features from the augmented image, thereby enhancing the perception capabilities of LVLMs and effectively mitigating object hallucinations. Extensive experiments over multiple generative and discriminative benchmarks show that AGLA achieves superior performance on hallucination mitigation as well as other perception tasks.

The contributions of this work can be summarized as threefold:

- We examine object hallucinations in LVLMs and identify the deficiency of attention toward images as the root cause. This finding offers a new view of object hallucinations and opens a new door for understanding and mitigating hallucinations.
- We design *AGLA*, a training-free and plug-and-play decoding framework that ensembles prompt-independent global attention and prompt-dependent local attention to capture discriminative and generative image features simultaneously, greatly enhancing the perception ability of LVLMs.
- Extensive experiments over multiple generative and discriminative benchmarks show that *AGLA* achieves superior performance in hallucination mitigation.

2 Related Work

2.1 Large Vision-Language Models

Benefiting from the rapid development of Large Language Models (LLMs) [38, 2, 39, 40, 1, 41, 5, 4, 3], Large Vision-Language Models (LVLMs) [6, 10, 7, 9, 8, 12] have also made great strides by incorporating visual encoders and feature projectors [42, 43, 44, 45], marking a significant enhancement in their performance and adaptability on various multimodal tasks [13, 14, 15, 16, 46]. Most of the LVLMs share the same two training phases, i.e., pre-training for feature alignment and instruction-based LLM fine-tuning [42, 45, 10]. Furthermore, recent research efforts also attempt to enhance the alignment between model responses and human values through Reinforcement Learning from Human Feedback (RLHF) [47] and preference fine-tuning [48]. Despite the rapid development, similar to LLMs, LVLMs are prone to generating hallucinations [49, 50, 51], which significantly impacts their reliability and stability for real-world applications.

2.2 Object Hallucination

Hallucination [52, 53, 54] in the NLP community is defined as the generation of incorrect or nonsensical content. Recently, this issue has also attracted much attention in the multimodal domain. Among different kinds of multimodal hallucinations [20], “object hallucination” is most precisely defined and widely studied, referring to LVLMs generating responses that include objects not present in images [49, 55, 24, 50, 24, 18]. Previous researches have shown that object hallucination may come from the statistical bias of pre-training [25, 26, 27], over-reliance on parametric knowledge [19, 28, 29, 30, 31] and biased feature learning [22, 32, 33]. Despite these efforts, more underlying reasons for object hallucinations are still under-explored. To mitigate object hallucinations, previous work usually introduces multimodal instruction tuning [23, 56, 57, 17, 58], trains a post-hoc reviser [59, 60, 61] or designs specific decoding strategies [32, 19, 22, 62]. To be more specific, Woodpecker [60] utilizes ChatGPT [1] to revise the generated responses. DOLA [62] contrasts the differences in logits obtained from the later and earlier layers of LVLMs to reduce hallucinations. OPERA [32] proposes a penalty-based decoding method equipped with a retrospection-reallocation strategy to penalize candidates that may lead to hallucinations. VCD [19] extends contrastive decoding in NLP [63, 64] into the multimodal domain by contrasting outputs from original and distorted images.

3 Preliminary Study

In this section, we start from an intuitive observation and pinpoint possible causes of object hallucinations as well as potential solutions that could mitigate object hallucinations.

Observation. Identifying when LVLMs are prone to generating object hallucinations is critical for mitigating this problem. To this end, we examine and observe that the ratio of object hallucinations increases with the number of objects in the image increases, as illustrated in Fig. 3 (a). Though prior studies [65, 66] have pointed out that the complexity of images can affect the performance of visual grounding, it remains unclear why it makes LVLMs more susceptible to object hallucinations.

Hallucination via Association. We speculate that the increasing number of objects leads to more hallucinations because LVLMs can be easily disturbed by various objects in images. To verify this

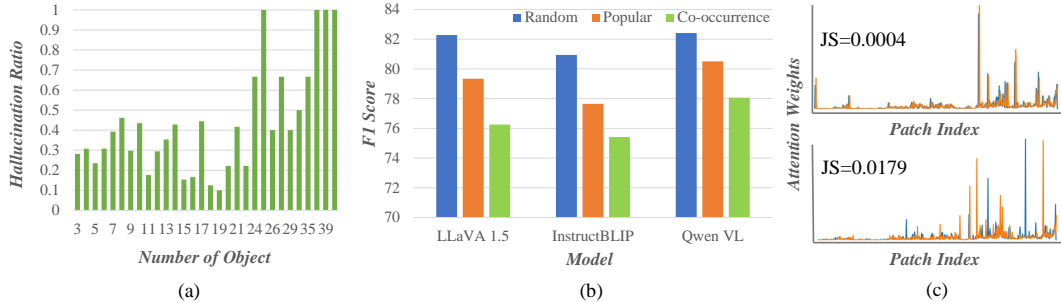


Figure 3: (a) Hallucination ratio with different numbers of objects in the image over the POPE dataset. (b) Model performance with different types of hallucinated objects over the POPE dataset. (c) Attention distribution toward original images (Top) and augmented images (Bottom) with existent (orange) and non-existent (blue) object queries and their Jensen–Shannon (JS) divergence.

hypothesis, we further conduct statistical analysis on the types of hallucinated objects. As Fig. 3 (b) shows, compared with random and popular objects, LVLMs are more likely to hallucinate objects that co-appear frequently in images (a lower F1 score means a higher hallucination rate). This study reveals that LVLMs can be easily affected by various objects in images and tend to generate hallucinations via object association (e.g., hallucinating “cups” through “table” in images), largely due to the statistical bias in LVM pre-training [25, 26, 27]. Furthermore, the vulnerability of LVLMs to interference from the increasing objects suggests that these models attempt to understand the global content in images and model attention toward prompt-relevant local context may diminish with the growing objects, which makes the association bias overwhelm the diminished local attention and leads to object hallucinations.

Attention Deficiency. To verify that LVLMs predominantly attend to global image features while failing to capture prompt-relevant local features, we visualize the self-attention weights of LVLMs toward image patch features in the top graph of Fig. 3 (c). We can observe that the attention is dominated by certain global features and presents a similar pattern regardless of queried objects being present (orange curve) or absent (blue curve) in images. This study reveals that LVLMs tend to focus on certain prompt-independent global features instead of prompt-dependent local features. Such a tendency toward global features makes LVLMs susceptible to interference by existing objects in the image and generating hallucinations through association.

Solution. One viable way of mitigating hallucinations is to incorporate prompt-dependent local attention to mitigate the *attention deficiency* in LVLMs. This could be achieved by masking out distracting content and forcing LVLMs to focus on prompt-dependent local image regions. We verify it in the bottom graph of Fig. 3 (c), where LVLMs produce clearly different attention for the augmented views when they receive different queried objects being present (orange curve) or absent (blue curve) in the image. Hence, one possible solution is to feed LVLMs with the original input image to avoid information loss as well as its augmented view to capture local prompt-dependent features simultaneously. More details about generating the augmented image view and incorporating it to complement the original image will be elaborated in the ensuing subsections.

4 Method

To direct LVLMs’ focus to image regions relevant to prompts and mask out distractions, we propose an *Image-Prompt Matching (IPM)* technique to generate an augmented view of the input image (Sec. 4.1). Building on this, we introduce the *Assembly of Global and Local Attention (AGLA)*, which integrates generative global features from original images with discriminative local features from augmented images, thereby deriving a calibrated distribution for more accurate decoding (Sec. 4.2).

4.1 Image-Prompt Matching

Large Vision-Language Models (LVLMs) often fail to focus on image regions relevant to input prompts due to *attention deficiency*. To address this issue, we introduce an *Image-Prompt Matching (IPM)* module (illustrated in Fig. 4) to identify and mask out irrelevant image regions, ensuring that LVLMs focus on prompt-relevant content. This module calculates an overall similarity score,

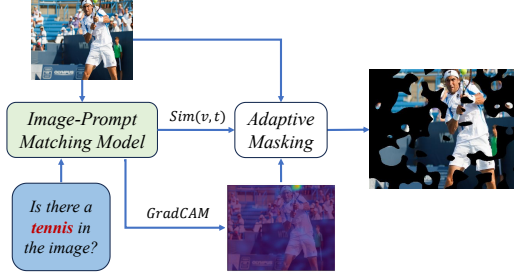


Figure 4: An illustration of the proposed Image-Prompt Matching (IPM) module.

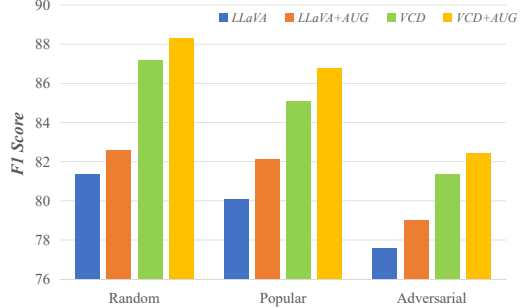


Figure 5: Model performance with original and augmented (+AUG) images.

$sim(v, t)$, between the image v and the textual prompt t . Leveraging advancements in interpretability techniques, we adopt GradCAM [36, 37] and apply it to the cross-attention layer of the matching model, yielding a correlation score for each image patch relative to the input prompts. Specifically, let $X \in \mathbb{R}^{M \times D_t}$ represent the prompt token features and $Y \in \mathbb{R}^{K \times D_v}$ represent the image patch features (M and K denote the number of prompt tokens and image patches, respectively). The cross-attention matrix $C \in \mathbb{R}^{M \times K}$ can be computed as follows:

$$C = \text{softmax} \left(\frac{XW_TW_V^T Y^T}{\sqrt{D_t}} \right) \quad (1)$$

where $W_T \in \mathbb{R}^{D_t \times D_t}$ and $W_V \in \mathbb{R}^{D_v \times D_t}$ denote parameters of the cross-attention heads. D_t and D_v denote the dimensions of prompt token and image patch features, respectively. The cross-attention matrix C quantifies the attention each prompt token allocates to each image patch, with C_{ij} representing the attention between the i -th prompt token and the j -th image patch. The correlation score for the j -th image patch with respect to the entire textual prompt can thus be computed as follows:

$$\text{cor}(j) = \frac{1}{H} \sum_{i=1}^M \sum_{h=1}^H \max \left(0, \frac{\partial \text{sim}(v, t)}{\partial C_{ij}^{(h)}} \right) C_{ij}^{(h)} \quad (2)$$

where H denotes the number of cross-attention heads, and $C^{(h)}$ is the cross-attention matrix for the h -th head. The partial derivative term measures the sensitivity of the similarity score to the cross-attention score, indicating the importance of each attention. This process allows computing the correlation score for each image patch and identifying those most relevant to the input prompts.

To ensure LVLMs focus on prompt-relevant image content while blocking out distraction objects, we introduce an adaptive masking strategy based on the computed correlation scores. This strategy masks out image regions with low correlation scores while retaining those with high scores. We determine the ratio of masking adaptively based on the overall similarity score $sim(v, t)$, instead of using a manually-defined ratio for all images and prompts. Specifically, we simply adopt $sim(v, t)/2$ as the masking ratio, allowing the masking process to adapt to varying levels of image-prompt matching. For image-prompt pairs with higher similarity scores, indicating a higher relevance between the image and prompt, a larger portion of the image will be masked out for effective distraction suppression and hallucination mitigation.

Validation. With the help of the matching model, LVLMs can focus on image regions corresponding to the prompt and capture prompt-dependent local features, thereby alleviating the *attention deficiency* issue. To validate the effectiveness of the proposed IPM module, we perform experiments on the POPE [24] dataset. As shown in Fig. 5, LLaVA [6] and the SOTA method VCD [19] both perform better by simply replacing original images with augmented images from IPM, demonstrating the effectiveness of IPM in distraction suppression and hallucination mitigation.

4.2 Assembly of Global and Local Attention

While IPM effectively blocks out distractions and captures crucial local features for visual discrimination, it inevitably introduces information loss because it blocks out some global features that are essential for generative tasks. To address this, we design AGLA that integrates local and global

attention to capture both discriminative and generative features, thereby learning more comprehensive image representations. Specifically, at each decoding step i , we assemble the logits derived from both the original and augmented images to obtain a calibrated decoding distribution. This assemble strategy can be formulated as follows:

$$p_{AGLA}(y_i | v, v^{aug}, t, y_{<i}) \sim \text{softmax}[\text{logit}_\theta(y_i | v, t, y_{<i}) + \alpha \text{logit}_\theta(y_i | v^{aug}, t, y_{<i})] \quad (3)$$

where y_i denotes the token at decoding step i , and $y_{<i}$ represents the sequence of generated tokens before step i . The variables v , v^{aug} , and t denote the original image, the augmented image, and the input prompt, respectively. The parameter θ denotes the model parameters of the LVLMs, and α is a weighting coefficient that balances the contributions of local and global features.

Adaptive Plausibility Constraints.

Previous works [63, 19, 22] suggest that calibrating the entire output distribution, as in Eq. 3, may penalize valid outputs from the original distribution and promote implausible outputs from the augmented distribution. To mitigate this issue, we adopt adaptive plausibility constraints [63] to selectively consider tokens with high original probabilities and truncate other tokens as follows:

$$\begin{aligned} \mathcal{V}_{\text{token}}(y_{<i}) &= \{y_i \in \mathcal{V} : p_\theta(y_i | v, t, y_{<i}) \geq \beta \max_w p_\theta(w | v, t, y_{<i})\} \\ p_{AGLA}(y_i | v, v^{aug}, t, y_{<i}) &= 0, \text{ if } y_i \notin \mathcal{V}_{\text{token}}(y_{<i}), \end{aligned} \quad (4)$$

where $\mathcal{V}_{\text{token}}$ is the set of selected tokens and \mathcal{V} is the output vocabulary. β is a hyper-parameter that controls the strength of truncation. A larger β means only high-probability tokens will be retained.

Understanding from the Temperature Perspective. The proposed integration strategy can be interpreted as applying adaptive sampling temperatures [67] during decoding. For similar predictions from the original and augmented images, the integration effectively sets a lower temperature for the original logits, skewing the distribution towards high-probability tokens and avoiding the selection of low-probability tokens. Conversely, for dissimilar predictions, the integration works like setting a higher temperature, making the distribution closer to uniform, and thus increasing the likelihood of sampling correct tokens by giving more balanced consideration to various tokens.

5 Experiments

5.1 Experimental Settings

Datasets. We evaluate our model on both discriminative and generative datasets as listed below. More details about the datasets are provided in Appendix A2.

POPE: The Polling-based Object Probing Evaluation [24] contains 27,000 Yes/No questions about object existence in three datasets: MSCOCO [68], A-OKVQA [69], and GQA [70]. Each dataset includes three negative sample settings: random, popular, and adversarial. The evaluation metrics include Accuracy, Precision, Recall, and F1 score.

MME [71]: This comprehensive benchmark assesses the overall ability of LVLMs, with performance evaluated via the total score of Accuracy and Accuracy+.

CHAIR: Caption Hallucination Assessment with Image Relevance (CHAIR) [49] quantifies object hallucinations in image captions by comparing generated objects to ground-truth objects. Following previous works [32, 33], we randomly select 100 images from the MSCOCO dataset [68] and use CHAIR_I, CHAIR_S, and Recall as evaluation metrics.

LLaVA-Bench-Wild [6]: This dataset contains 24 images with 60 questions to assess the capability of LVLMs in tackling challenging tasks and their adaptability to new domains. Following previous work [19, 32], we use GPT-4 to evaluate the accuracy and detailedness of generated captions. The prompt and an example for GPT-4 evaluation are shown in Appendix A7.

Implementation Details. We evaluate the effectiveness of our model on two state-of-the-art LVLMs: LLaVA 1.5 [6] and InstructBLIP [10], with Vicuna 7B as language decoder and multinomial sampling as the decoding strategy (denoted as Regular). We also compare our model with three state-of-the-art models: OPERA [32], DOLA [62] and VCD [19]. We use BLIP-ITM [45] as the Image-Prompt Matching model. We report average results over 3 runs on all benchmarks. For compared models, we follow the suggested settings in their respective papers and released codes to ensure a fair comparison. More details are provided in Appendix A3.

Table 1: Experimental results on POPE. Results for Regular and VCD are cited from [19].

Setting	Model	Decoding	Accuracy	Precision	Recall	F1 Score
Random	LLaVA1.5	Regular	83.49	88.84	76.76	82.28
		DOLA	84.78	87.59	81.27	84.19
		OPERA	87.53	94.52	79.80	86.45
		VCD	86.84	87.15	86.68	86.83
		AGLA	88.54	94.41	82.08	87.71
	InstructBLIP	Regular	80.42	78.93	83.21	80.94
		DOLA	83.00	83.06	83.13	83.00
		OPERA	85.07	88.39	80.73	84.39
		VCD	84.11	84.20	85.36	84.13
		AGLA	87.30	88.83	85.68	87.07
Popular	LLaVA1.5	Regular	79.98	82.47	76.76	79.34
		DOLA	79.75	84.11	76.22	80.61
		OPERA	84.21	88.00	79.80	83.50
		VCD	82.65	87.15	80.59	83.37
		AGLA	85.14	87.88	82.08	84.68
	InstructBLIP	Regular	76.09	73.22	82.94	77.65
		DOLA	78.99	77.12	83.13	79.85
		OPERA	78.33	73.85	87.73	80.20
		VCD	79.94	77.84	83.33	80.80
		AGLA	81.86	80.17	85.68	82.58
Adversarial	LLaVA1.5	Regular	76.03	76.11	76.80	76.26
		DOLA	76.32	77.27	75.47	76.16
		OPERA	80.88	82.16	79.76	80.69
		VCD	77.31	73.43	86.47	79.28
		AGLA	81.13	81.20	82.10	81.36
	InstructBLIP	Regular	72.37	68.78	83.06	75.42
		DOLA	74.67	71.53	83.11	76.68
		OPERA	75.50	70.49	87.73	78.17
		VCD	76.32	73.24	84.08	78.08
		AGLA	77.29	74.09	85.67	79.16

5.2 Experimental Results

Experiments on POPE. Table 1 shows average experimental results on the three POPE datasets [24] under the random, popular, and adversarial settings. It is obvious that AGLA consistently outperforms the regular decoding strategy by substantial margins (average improvements of 5.5% in accuracy and 5.1% in F1 score) across all LVLMS and experimental settings. Additionally, AGLA surpasses state-of-the-art decoding methods clearly, demonstrating its effectiveness in mitigating object hallucinations. Furthermore, the improved performance in the adversarial (i.e., co-occurrence) setting confirms that our model effectively resolves *attention deficiency* and mitigates object hallucinations caused by object association, aligning with our analysis in Sec. 3. Detailed experimental results are provided in Appendix A4 and model comparison with different decoding strategies is detailed in Appendix A5.

Experiments on MME Hallucination Subset. Beyond object hallucination evaluation on the POPE dataset, we conduct comprehensive experiments on the MME hallucination subset, which includes four types of hallucinations. As illustrated in Fig. 6 and 7, the proposed model consistently outperforms both regular and SOTA decoding strategies across all hallucination categories and LVLMS. This underscores AGLA’s effectiveness in addressing a broader range of multimodal hallucination challenges beyond objects. To further evaluate the impact of AGLA on the overall capabilities of LVLMS, we also conduct experiments on MME perception-related datasets, as presented in Table A3 in the Appendix. The improved performance in these experiments further validates the effectiveness of AGLA in enhancing the general perception capabilities of LVLMS.

Results on Open-ended Generation with CHAIR Evaluation. Beyond the “Yes-or-No” discriminative evaluations on the POPE and MME datasets, we also validate our model on open-ended caption generation using the CHAIR benchmark [49]. The results in Table 2 demonstrate consistent improvements in our model over the compared methods. Specifically, AGLA effectively reduces object hallucinations in generated captions, as evidenced by lower CHAIR_S and CHAIR_I scores.

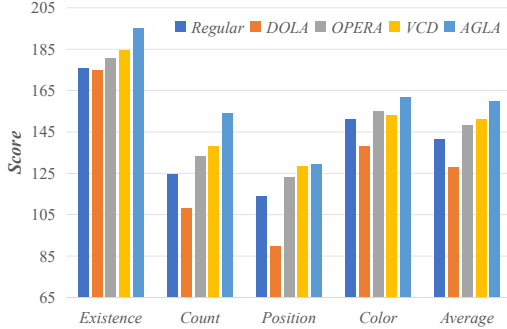


Figure 6: Model performance on MME hallucination subset with LLaVA-1.5.

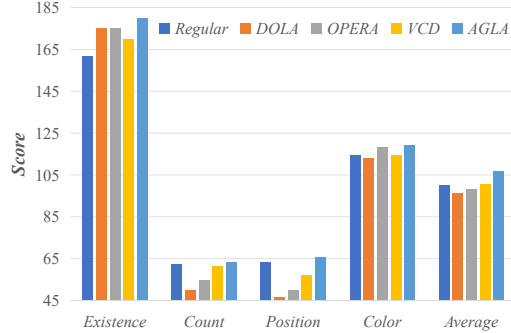


Figure 7: Model performance on MME hallucination subset with InstructBLIP.

Table 2: Results on the subset of CHAIR.

Model	Decoding	CHAIR _S ↓	CHAIR _T ↓	Recall ↑	Avg. Len
LLaVA1.5	Regular	51.0	15.2	75.2	102.2
	DOLA	57.0	15.9	78.2	97.5
	VCD	51.0	14.9	77.2	101.9
	OPERA	47.0	14.6	78.5	95.3
	AGLA	43.0	14.1	78.9	98.8
InstructBLIP	Regular	54.0	18.1	71.1	115.3
	DOLA	60.0	20.1	71.5	110.8
	VCD	57.0	17.0	72.1	112.1
	OPERA	54.0	12.8	69.8	93.6
	AGLA	49.0	12.1	72.5	104.4

In addition, AGLA also enhances the detailedness of the generated captions, as indicated by higher Recall scores. In summary, AGLA achieves a good balance between accuracy and detailedness in open-ended caption generation, benefiting from the integration of discriminative local features and generative global features.

Qualitative Results. In addition to quantitative analysis, we present qualitative examples of different decoding methods in Fig. 8. Regular decoding [6] and VCD [19] often produce object hallucinations, especially in the latter part of their outputs. These issues are attributed to *attention deficiency* and association bias, such as hallucinating “backpack” and “car” based on “person”. In contrast, our model effectively mitigates these issues by masking out distractions in the image to mitigate association bias and assembling local and global image features to avoid attention deficiency. Additional qualitative examples are provided in the Appendix A8.

GPT-4 Aided Evaluation. Beyond the object-level evaluation on CHAIR [49], we use GPT-4 to assess the overall quality of the generated captions on the LLaVA-Bench-Wild dataset, following previous works [32, 19]. Experimental results in Table 3 show that our model outperforms other methods across all evaluation metrics. Specifically, the improved accuracy indicates that AGLA effectively mitigates hallucinations in the generated captions by incorporating local and global image attention. Additionally, the enhancement in detailedness highlights AGLA’s ability to improve the global perceptual capabilities of LVLMs, enabling the generation of more comprehensive captions.

Ablation Study. To evaluate the effectiveness of each design in our model, we conduct an ablation study on the POPE-COCO dataset under the popular setting with LLaVA 1.5, as shown in Table 4. The performance degradation in the following different model variants demonstrates the importance of each design in our model: (1) *Truncation Removal*: Omitting truncation in Eq. 4 leads to performance drop. Adaptive plausibility constraints are crucial for preventing the calibrated distribution from deviating excessively from the original distribution, thus preserving essential global information. (2) *Fixed vs. Adaptive Masking Ratio*: Using a fixed masking ratio results in clearly degraded performance. A fixed ratio cannot accurately capture the model’s matching confidence for different image-prompt pairs. (3) *Without Assembly*: Relying solely on the augmented distribution degrades

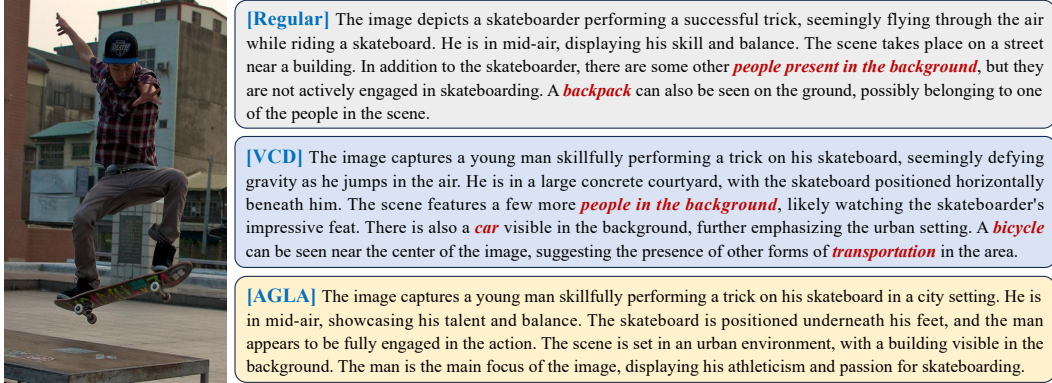


Figure 8: Illustration of generated captions by different decoding methods with LLaVA 1.5 as the backbone model. Hallucinated content is highlighted in *red*.

Table 3: Results of GPT-4-aided evaluation on the LLaVA-Bench-Wild dataset. Both metrics are scored on a scale of 10.

Model	Decoding	Acc. \uparrow	Detail. \uparrow
LLaVA1.5	Regular	2.61	3.65
	VCD	3.00	3.83
	DOLA	3.51	4.22
	OPERA	3.68	4.29
	AGLA	3.83	4.39
InstructBLIP	Regular	2.82	3.36
	DOLA	4.04	4.33
	VCD	4.50	4.55
	OPERA	4.56	4.48
	AGLA	4.59	4.59

Table 4: Ablation study with different model variants and masking strategies on POPE-COCO under the popular setting.

Model	Accuracy	F1
AGLA	86.12	84.71
<i>Model Variants</i>		
w/o Truncation	85.66	84.42
w/o Adaptive Ratio	84.83	82.94
w/o Assembly	83.53	82.14
Regular	81.88	80.06
<i>Masking Strategy</i>		
Patch	85.77	84.05
Soft	85.51	83.93
Feature	85.27	83.73
Random	83.56	82.40

the performance by large margins, as the original image distribution helps provide global image information. (4) *Comparison with Regular Decoding*: Despite the variations, each modified model variant outperforms regular decoding (Regular), demonstrating the overall effectiveness of our model. (5) *Masking Strategies*: We also test several masking strategies: Patch-level Masking (Patch) results in a slight performance drop due to its nature of coarse-grained masking. Soft Masking (Soft) using relevance scores as weights leads to performance decline, as the highly variable relevance values can cause important information to be masked. Feature-level Masking (Feature) leads to a performance drop because self-attention may cause masked information to leak. Despite the variations, each masking strategy performs much better than random masking (Random), highlighting the necessity of the matching model.

6 Conclusion

In this paper, we investigate the underlying reasons for object hallucinations in LVLMs, identifying attention deficiency as the root cause. To address this, we propose *Assembly of Global and Local Attention (AGLA)*, a training-free, plug-and-play approach that mitigates object hallucinations by combining local and global model attention to capture both discriminative and generative image features. Our approach features an image-prompt matching scheme that captures prompt-dependent local attention toward images, resulting in an augmented view of the input image where prompt-independent distractions are masked. We then integrate generative global features from original images with discriminative local features from augmented images to derive a calibrated decoding distribution, thereby enhancing the generation and perception capabilities of LVLMs. Experiments on various discriminative and generative benchmarks demonstrate that our model significantly reduces object hallucinations and improves the general perception capabilities of LVLMs.

Acknowledgments

This work was supported by National Science and Technology Major Project (2022ZD0117102), National Natural Science Foundation of China (62293551, 62177038, 62277042, 62137002, 61937001, 62377038). Project of China Knowledge Centre for Engineering Science and Technology, “LENOVO-XJTU” Intelligent Industry Joint Laboratory Project.

References

- [1] Tom Brown, Benjamin Mann, Nick Ryder, Melanie Subbiah, Jared D Kaplan, Prafulla Dhariwal, Arvind Neelakantan, Pranav Shyam, Girish Sastry, Amanda Askell, et al. Language models are few-shot learners. *Advances in neural information processing systems*, 33:1877–1901, 2020.
- [2] Hugo Touvron, Thibaut Lavril, Gautier Izacard, Xavier Martinet, Marie-Anne Lachaux, Timothée Lacroix, Baptiste Rozière, Naman Goyal, Eric Hambro, Faisal Azhar, et al. Llama: Open and efficient foundation language models. *arXiv preprint arXiv:2302.13971*, 2023.
- [3] Jinze Bai, Shuai Bai, Yunfei Chu, Zeyu Cui, Kai Dang, Xiaodong Deng, Yang Fan, Wenbin Ge, Yu Han, Fei Huang, et al. Qwen technical report. *arXiv preprint arXiv:2309.16609*, 2023.
- [4] Wei-Lin Chiang, Zhuohan Li, Zi Lin, Ying Sheng, Zhanghao Wu, Hao Zhang, Lianmin Zheng, Siyuan Zhuang, Yonghao Zhuang, Joseph E. Gonzalez, Ion Stoica, and Eric P. Xing. Vicuna: An open-source chatbot impressing gpt-4 with 90%* chatgpt quality, March 2023.
- [5] Rohan Taori, Ishaan Gulrajani, Tianyi Zhang, Yann Dubois, Xuechen Li, Carlos Guestrin, Percy Liang, and Tatsunori B. Hashimoto. Stanford alpaca: An instruction-following llama model, 2023.
- [6] Haotian Liu, Chunyuan Li, Qingyang Wu, and Yong Jae Lee. Visual instruction tuning. *arXiv preprint arXiv:2304.08485*, 2023.
- [7] Deyao Zhu, Jun Chen, Xiaoqian Shen, Xiang Li, and Mohamed Elhoseiny. Minigpt-4: Enhancing vision-language understanding with advanced large language models. *arXiv preprint arXiv:2304.10592*, 2023.
- [8] Qinghao Ye, Haiyang Xu, Guohai Xu, Jiabo Ye, Ming Yan, Yiyang Zhou, Junyang Wang, Anwen Hu, Pengcheng Shi, Yaya Shi, Chenliang Li, Yuanhong Xu, Hehong Chen, Junfeng Tian, Qian Qi, Ji Zhang, and Fei Huang. mplug-owl: Modularization empowers large language models with multimodality. *arXiv preprint arXiv:2304.14178*, 2023.
- [9] Bo Li, Yuanhan Zhang, Liangyu Chen, Jinghao Wang, Jingkang Yang, and Ziwei Liu. Otter: A multi-modal model with in-context instruction tuning. *arXiv preprint arXiv:2305.03726*, 2023.
- [10] Wenliang Dai, Junnan Li, Dongxu Li, Anthony Meng Huat Tiong, Junqi Zhao, Weisheng Wang, Boyang Li, Pascale Fung, and Steven Hoi. Instructblip: Towards general-purpose vision-language models with instruction tuning. *arXiv preprint arXiv:2306.04387*, 2023.
- [11] Tao Gong, Chengqi Lyu, Shilong Zhang, Yudong Wang, Miao Zheng, Qian Zhao, Kuikun Liu, Wenwei Zhang, Ping Luo, and Kai Chen. Multimodal-gpt: A vision and language model for dialogue with humans. *arXiv preprint arXiv:2305.04790*, 2023.
- [12] Jinze Bai, Shuai Bai, Shusheng Yang, Shijie Wang, Sinan Tan, Peng Wang, Junyang Lin, Chang Zhou, and Jingren Zhou. Qwen-vl: A frontier large vision-language model with versatile abilities. *arXiv preprint arXiv:2308.12966*, 2023.
- [13] Junnan Li, Dongxu Li, Silvio Savarese, and Steven Hoi. Blip-2: Bootstrapping language-image pre-training with frozen image encoders and large language models. *arXiv preprint arXiv:2301.12597*, 2023.
- [14] Teng Wang, Jinrui Zhang, Junjie Fei, Yixiao Ge, Hao Zheng, Yunlong Tang, Zhe Li, Mingqi Gao, Shanshan Zhao, Ying Shan, et al. Caption anything: Interactive image description with diverse multimodal controls. *arXiv preprint arXiv:2305.02677*, 2023.
- [15] Jusung Lee, Sungguk Cha, Younghyun Lee, and Cheoljong Yang. Visual question answering instruction: Unlocking multimodal large language model to domain-specific visual multitasks. *arXiv preprint arXiv:2402.08360*, 2024.

- [16] Haibo Wang, Chenghang Lai, Yixuan Sun, and Weifeng Ge. Weakly supervised gaussian contrastive grounding with large multimodal models for video question answering. *arXiv preprint arXiv:2401.10711*, 2024.
- [17] Fuxiao Liu, Kevin Lin, Linjie Li, Jianfeng Wang, Yaser Yacoob, and Lijuan Wang. Mitigating hallucination in large multi-modal models via robust instruction tuning. *arXiv preprint arXiv:2306.14565*, 2023.
- [18] Holy Lovenia, Wenliang Dai, Samuel Cahyawijaya, Ziwei Ji, and Pascale Fung. Negative object presence evaluation (nope) to measure object hallucination in vision-language models. *arXiv preprint arXiv:2310.05338*, 2023.
- [19] Sicong Leng, Hang Zhang, Guanzheng Chen, Xin Li, Shijian Lu, Chunyan Miao, and Lidong Bing. Mitigating object hallucinations in large vision-language models through visual contrastive decoding. *arXiv preprint arXiv:2311.16922*, 2023.
- [20] Hanchao Liu, Wenyuan Xue, Yifei Chen, Dapeng Chen, Xiutian Zhao, Ke Wang, Liping Hou, Rongjun Li, and Wei Peng. A survey on hallucination in large vision-language models. *arXiv preprint arXiv:2402.00253*, 2024.
- [21] Ailin Deng, Zhirui Chen, and Bryan Hooi. Seeing is believing: Mitigating hallucination in large vision-language models via clip-guided decoding. *arXiv preprint arXiv:2402.15300*, 2024.
- [22] Lanyun Zhu, Deyi Ji, Tianrun Chen, Peng Xu, Jieping Ye, and Jun Liu. Ibid: Alleviating hallucinations in large vision-language models via image-biased decoding. *arXiv preprint arXiv:2402.18476*, 2024.
- [23] Anisha Gunjal, Jihan Yin, and Erhan Bas. Detecting and preventing hallucinations in large vision language models. *arXiv preprint arXiv:2308.06394*, 2023.
- [24] Yifan Li, Yifan Du, Kun Zhou, Jinpeng Wang, Wayne Xin Zhao, and Ji-Rong Wen. Evaluating object hallucination in large vision-language models. *arXiv preprint arXiv:2305.10355*, 2023.
- [25] Vedika Agarwal, Rakshith Shetty, and Mario Fritz. Towards causal vqa: Revealing and reducing spurious correlations by invariant and covariant semantic editing. In *Proceedings of the IEEE/CVF Conference on Computer Vision and Pattern Recognition*, pages 9690–9698, 2020.
- [26] Aishwarya Agrawal, Dhruv Batra, and Devi Parikh. Analyzing the behavior of visual question answering models. *arXiv preprint arXiv:1606.07356*, 2016.
- [27] Yash Goyal, Tejas Khot, Douglas Summers-Stay, Dhruv Batra, and Devi Parikh. Making the v in vqa matter: Elevating the role of image understanding in visual question answering. In *Proceedings of the IEEE conference on computer vision and pattern recognition*, pages 6904–6913, 2017.
- [28] Seongyun Lee, Sue Hyun Park, Yongrae Jo, and Minjoon Seo. Volcano: mitigating multimodal hallucination through self-feedback guided revision. *arXiv preprint arXiv:2311.07362*, 2023.
- [29] Ren Zhibo, Wang Huizhen, Zhu Muhua, Wang Yichao, Xiao Tong, and Zhu Jingbo. Overcoming language priors with counterfactual inference for visual question answering. In *Proceedings of the 22nd Chinese National Conference on Computational Linguistics*, pages 600–610, 2023.
- [30] Yudong Han, Liqiang Nie, Jianhua Yin, Jianlong Wu, and Yan Yan. Visual perturbation-aware collaborative learning for overcoming the language prior problem. *arXiv preprint arXiv:2207.11850*, 2022.
- [31] Yike Wu, Yu Zhao, Shiwan Zhao, Ying Zhang, Xiaojie Yuan, Guoqing Zhao, and Ning Jiang. Overcoming language priors in visual question answering via distinguishing superficially similar instances. *arXiv preprint arXiv:2209.08529*, 2022.
- [32] Qidong Huang, Xiaoyi Dong, Pan Zhang, Bin Wang, Conghui He, Jiaqi Wang, Dahua Lin, Weiming Zhang, and Nenghai Yu. Opera: Alleviating hallucination in multi-modal large language models via over-trust penalty and retrospection-allocation. *arXiv preprint arXiv:2311.17911*, 2023.
- [33] Zihao Yue, Liang Zhang, and Qin Jin. Less is more: Mitigating multimodal hallucination from an eos decision perspective. *arXiv preprint arXiv:2402.14545*, 2024.
- [34] Leila Kabbai, Mehrez Abdellaoui, and Ali Douik. Image classification by combining local and global features. *The Visual Computer*, 35:679–693, 2019.

- [35] Namuk Park, Wonjae Kim, Byeongho Heo, Taekyung Kim, and Sangdoon Yun. What do self-supervised vision transformers learn? *arXiv preprint arXiv:2305.00729*, 2023.
- [36] Ramprasaath R Selvaraju, Michael Cogswell, Abhishek Das, Ramakrishna Vedantam, Devi Parikh, and Dhruv Batra. Grad-cam: Visual explanations from deep networks via gradient-based localization. In *Proceedings of the IEEE international conference on computer vision*, pages 618–626, 2017.
- [37] Anthony Meng Huat Tiong, Junnan Li, Boyang Li, Silvio Savarese, and Steven CH Hoi. Plug-and-play vqa: Zero-shot vqa by conjoining large pretrained models with zero training. *arXiv preprint arXiv:2210.08773*, 2022.
- [38] Fabrizio Gilardi, Meysam Alizadeh, and Maël Kubli. Chatgpt outperforms crowd-workers for text-annotation tasks. *arXiv preprint arXiv:2303.15056*, 2023.
- [39] Yi Tay, Mostafa Dehghani, Vinh Q Tran, Xavier Garcia, Jason Wei, Xuezhi Wang, Hyung Won Chung, Dara Bahri, Tal Schuster, Steven Zheng, et al. U12: Unifying language learning paradigms. In *The Eleventh International Conference on Learning Representations*, 2022.
- [40] Colin Raffel, Noam Shazeer, Adam Roberts, Katherine Lee, Sharan Narang, Michael Matena, Yanqi Zhou, Wei Li, and Peter J Liu. Exploring the limits of transfer learning with a unified text-to-text transformer. *The Journal of Machine Learning Research*, 21(1):5485–5551, 2020.
- [41] Aakanksha Chowdhery, Sharan Narang, Jacob Devlin, Maarten Bosma, Gaurav Mishra, Adam Roberts, Paul Barham, Hyung Won Chung, Charles Sutton, Sebastian Gehrmann, et al. Palm: Scaling language modeling with pathways. *arXiv preprint arXiv:2204.02311*, 2022.
- [42] Liunian Harold Li, Mark Yatskar, Da Yin, Cho-Jui Hsieh, and Kai-Wei Chang. Visualbert: A simple and performant baseline for vision and language. *arXiv preprint arXiv:1908.03557*, 2019.
- [43] Chen Sun, Austin Myers, Carl Vondrick, Kevin Murphy, and Cordelia Schmid. Videobert: A joint model for video and language representation learning. In *Proceedings of the IEEE/CVF international conference on computer vision*, pages 7464–7473, 2019.
- [44] Jianfeng Wang, Zhengyuan Yang, Xiaowei Hu, Linjie Li, Kevin Lin, Zhe Gan, Zicheng Liu, Ce Liu, and Lijuan Wang. Git: A generative image-to-text transformer for vision and language. *arXiv preprint arXiv:2205.14100*, 2022.
- [45] Junnan Li, Dongxu Li, Caiming Xiong, and Steven Hoi. Blip: Bootstrapping language-image pre-training for unified vision-language understanding and generation. In *International Conference on Machine Learning*, pages 12888–12900. PMLR, 2022.
- [46] Haonan Lin, Mengmeng Wang, Yan Chen, Wenbin An, Yuzhe Yao, Guang Dai, Qianying Wang, Yong Liu, and Jingdong Wang. Dreamsalon: A staged diffusion framework for preserving identity-context in editable face generation. *arXiv preprint arXiv:2403.19235*, 2024.
- [47] Zhiqing Sun, Sheng Shen, Shengcao Cao, Haotian Liu, Chunyuan Li, Yikang Shen, Chuang Gan, Liang-Yan Gui, Yu-Xiong Wang, Yiming Yang, et al. Aligning large multimodal models with factually augmented rlhf. *arXiv preprint arXiv:2309.14525*, 2023.
- [48] Yiyang Zhou, Chenhang Cui, Rafael Rafailov, Chelsea Finn, and Huaxiu Yao. Aligning modalities in vision large language models via preference fine-tuning. *arXiv preprint arXiv:2402.11411*, 2024.
- [49] Anna Rohrbach, Lisa Anne Hendricks, Kaylee Burns, Trevor Darrell, and Kate Saenko. Object hallucination in image captioning. *arXiv preprint arXiv:1809.02156*, 2018.
- [50] Junyang Wang, Yiyang Zhou, Guohai Xu, Pengcheng Shi, Chenlin Zhao, Haiyang Xu, Qinghao Ye, Ming Yan, Ji Zhang, Jihua Zhu, et al. Evaluation and analysis of hallucination in large vision-language models. *arXiv preprint arXiv:2308.15126*, 2023.
- [51] Jiahao Nie, Gongjie Zhang, Wenbin An, Yap-Peng Tan, Alex C Kot, and Shijian Lu. Mmrel: A relation understanding dataset and benchmark in the mllm era. *arXiv preprint arXiv:2406.09121*, 2024.
- [52] Ziwei Ji, Nayeon Lee, Rita Frieske, Tiezheng Yu, Dan Su, Yan Xu, Etsuko Ishii, Ye Jin Bang, Andrea Madotto, and Pascale Fung. Survey of hallucination in natural language generation. *ACM Computing Surveys*, 55(12):1–38, 2023.

- [53] Yue Zhang, Yafu Li, Leyang Cui, Deng Cai, Lemao Liu, Tingchen Fu, Xinting Huang, Enbo Zhao, Yu Zhang, Yulong Chen, et al. Siren’s song in the ai ocean: A survey on hallucination in large language models. *arXiv preprint arXiv:2309.01219*, 2023.
- [54] Weijia Shi, Sewon Min, Michihiro Yasunaga, Minjoon Seo, Rich James, Mike Lewis, Luke Zettlemoyer, and Wen-tau Yih. Replug: Retrieval-augmented black-box language models. *arXiv preprint arXiv:2301.12652*, 2023.
- [55] Ali Furkan Biten, Lluís Gómez, and Dimosthenis Karatzas. Let there be a clock on the beach: Reducing object hallucination in image captioning. In *Proceedings of the IEEE/CVF Winter Conference on Applications of Computer Vision*, pages 1381–1390, 2022.
- [56] Lei Li, Yuwei Yin, Shicheng Li, Liang Chen, Peiyi Wang, Shuhuai Ren, Mukai Li, Yazheng Yang, Jingjing Xu, Xu Sun, et al. A large-scale dataset towards multi-modal multilingual instruction tuning. *arXiv preprint arXiv:2306.04387*, 2023.
- [57] Fuxiao Liu, Kevin Lin, Linjie Li, Jianfeng Wang, Yaser Yacoob, and Lijuan Wang. Aligning large multi-modal model with robust instruction tuning. *arXiv preprint arXiv:2306.14565*, 2023.
- [58] Zhiyang Chen, Yousong Zhu, Yufei Zhan, Zhaowen Li, Chaoyang Zhao, Jinqiao Wang, and Ming Tang. Mitigating hallucination in visual language models with visual supervision. *arXiv preprint arXiv:2311.16479*, 2023.
- [59] Yiyang Zhou, Chenhang Cui, Jaehong Yoon, Linjun Zhang, Zhun Deng, Chelsea Finn, Mohit Bansal, and Huaxiu Yao. Analyzing and mitigating object hallucination in large vision-language models. *arXiv preprint arXiv:2310.00754*, 2023.
- [60] Shukang Yin, Chaoyou Fu, Sirui Zhao, Tong Xu, Hao Wang, Dianbo Sui, Yunhang Shen, Ke Li, Xing Sun, and Enhong Chen. Woodpecker: Hallucination correction for multimodal large language models. *arXiv preprint arXiv:2310.16045*, 2023.
- [61] Junfei Wu, Qiang Liu, Ding Wang, Jinghao Zhang, Shu Wu, Liang Wang, and Tieniu Tan. Logical closed loop: Uncovering object hallucinations in large vision-language models. *arXiv preprint arXiv:2402.11622*, 2024.
- [62] Yung-Sung Chuang, Yujia Xie, Hongyin Luo, Yoon Kim, James Glass, and Pengcheng He. Dola: Decoding by contrasting layers improves factuality in large language models. *arXiv preprint arXiv:2309.03883*, 2023.
- [63] Xiang Lisa Li, Ari Holtzman, Daniel Fried, Percy Liang, Jason Eisner, Tatsunori Hashimoto, Luke Zettlemoyer, and Mike Lewis. Contrastive decoding: Open-ended text generation as optimization. *arXiv preprint arXiv:2210.15097*, 2022.
- [64] Sean O’Brien and Mike Lewis. Contrastive decoding improves reasoning in large language models. *arXiv preprint arXiv:2309.09117*, 2023.
- [65] Bryan A Plummer, Liwei Wang, Chris M Cervantes, Juan C Caicedo, Julia Hockenmaier, and Svetlana Lazebnik. Flickr30k entities: Collecting region-to-phrase correspondences for richer image-to-sentence models. In *Proceedings of the IEEE international conference on computer vision*, pages 2641–2649, 2015.
- [66] Ranjay Krishna, Yuke Zhu, Oliver Groth, Justin Johnson, Kenji Hata, Joshua Kravitz, Stephanie Chen, Yannis Kalantidis, Li-Jia Li, David A Shamma, et al. Visual genome: Connecting language and vision using crowdsourced dense image annotations. *International journal of computer vision*, 123:32–73, 2017.
- [67] Ari Holtzman, Jan Buys, Li Du, Maxwell Forbes, and Yejin Choi. The curious case of neural text degeneration. *arXiv preprint arXiv:1904.09751*, 2019.
- [68] Tsung-Yi Lin, Michael Maire, Serge Belongie, James Hays, Pietro Perona, Deva Ramanan, Piotr Dollár, and C Lawrence Zitnick. Microsoft coco: Common objects in context. In *Computer Vision—ECCV 2014: 13th European Conference, Zurich, Switzerland, September 6-12, 2014, Proceedings, Part V 13*, pages 740–755. Springer, 2014.
- [69] Dustin Schwenk, Apoorv Khandelwal, Christopher Clark, Kenneth Marino, and Roozbeh Mottaghi. A-okvqa: A benchmark for visual question answering using world knowledge. In *European Conference on Computer Vision*, pages 146–162. Springer, 2022.
- [70] Drew A Hudson and Christopher D Manning. Gqa: A new dataset for real-world visual reasoning and compositional question answering. In *Proceedings of the IEEE/CVF conference on computer vision and pattern recognition*, pages 6700–6709, 2019.

- [71] Chaoyou Fu, Peixian Chen, Yunhang Shen, Yulei Qin, Mengdan Zhang, Xu Lin, Zhenyu Qiu, Wei Lin, Jinrui Yang, Xiawu Zheng, et al. Mme: A comprehensive evaluation benchmark for multimodal large language models. *arXiv preprint arXiv:2306.13394*, 2023.
- [72] Jean-Baptiste Alayrac, Jeff Donahue, Pauline Luc, Antoine Miech, Iain Barr, Yana Hasson, Karel Lenc, Arthur Mensch, Katherine Millican, Malcolm Reynolds, et al. Flamingo: a visual language model for few-shot learning. *Advances in Neural Information Processing Systems*, 35:23716–23736, 2022.
- [73] Angela Fan, Mike Lewis, and Yann Dauphin. Hierarchical neural story generation. *arXiv preprint arXiv:1805.04833*, 2018.
- [74] Ronald A DeVore and Vladimir N Temlyakov. Some remarks on greedy algorithms. *Advances in computational Mathematics*, 5(1):173–187, 1996.
- [75] David H Ackley, Geoffrey E Hinton, and Terrence J Sejnowski. A learning algorithm for boltzmann machines. *Cognitive science*, 9(1):147–169, 1985.

Appendix

A1 Limitation and Future Work

Despite the superb performance in mitigating hallucinations and enhancing the general perception capabilities of LVLMs, our work could be improved in several aspects. First, we conducted experiments on the most widely used LVLMs (i.e., LLaVA 1.5 and InstructBLIP 7B) due to resource constraints. It will be useful to evaluate our model on larger LVLMs such as LLaVA 13B and Flamingo 70B [72]. In addition, this work focuses on text and image data. It could be extended to data from other modalities such as videos. We will examine these problems in our future work.

A2 Evaluation Metrics

The details of evaluation metrics for different datasets are listed below.

POPE. Since the output of the model for the POPE dataset [24] is limited to two types (Yes or No), it is convenient to measure the model performance with binary classification metrics: Accuracy, Precision, Recall, and F1 score.

MME. Similar to the POPE dataset, the MME dataset [71] contains only two types (Yes or No) of answers. Following the setting in their original paper, we use the sum of accuracy and accuracy+ as the final score, where accuracy is calculated based on each question and accuracy+ is calculated based on each image where both of the two questions need to be answered correctly. So accuracy+ is a stricter measurement that can better reflect the comprehensive understanding degree of the model.

CHAIR. Different from discriminative datasets like POPE and MME, CHAIR [49] (i.e., Caption Hallucination Assessment with Image Relevance) is a framework that quantifies object hallucinations for generative datasets. The sentence-level score $CHAIR_S$ represents the proportion of generated captions that contain hallucinations, while the instance-level score $CHAIR_I$ denotes the proportion of hallucinated objects relative to all mentioned objects in the generated captions. In addition, we also evaluate the semantic detailedness of generated captions with the metric Recall. $CHAIR_S$, $CHAIR_I$, and Recall are computed as follows.

$$C_S = \frac{|\{\text{Captions with hallucinated objects}\}|}{|\{\text{All captions}\}|}, C_I = \frac{|\{\text{Hallucinated objects}\}|}{|\{\text{All mentioned objects}\}|}, Recall = \frac{|\{\text{Accurate objects}\}|}{|\{\text{Ground-truth objects}\}|} \tag{A1}$$

LLaVA-Bench-Wild. LLaVA-Bench-Wild contains 24 images with 60 questions to assess the capability of LVLMs in tackling challenging tasks and their adaptability to new domains. Following previous works [32, 19], we use GPT-4 to evaluate the accuracy and detailedness of the generated captions. Specifically, the metric Accuracy measures the captions’ alignment with the image content and the metric Detailedness gauges the richness of details in the generated captions. The specific configurations used to prompt GPT-4 are listed in Table A4.

A3 Experimental Settings

For generative tasks on the CHAIR [49] and LLaVA-Bench-Wild [6] dataset, we set α to 1 and β to 0.1. Since the matching model cannot provide meaningful confidence in the relevance between general prompts (e.g., please describe this image in detail) and images for generative tasks, we simply use a fixed masking ratio of 0.1 to avoid information loss. For the POPE [24] dataset, α is set to 2 and β is set to 0.5. For the MME [71] dataset, we set α to 2 and β to 0.5 for LLaVA 1.5, while setting α and β to 0.1 for InstructBLIP. All experiments are conducted on a single RTX 3090 GPU.

A4 More Results on POPE

The results on the full POPE dataset [24] with three subsets (i.e., MSCOCO [68], A-OKVQA [69] and GQA [70]) and three negative sample settings (i.e., Random, Popular and Adversarial) are listed in Table A1. From the table, we can see that the proposed decoding strategy *AGLA* consistently outperforms the regular decoding strategy by large margins (average 5.5% accuracy and 5.1% F1

Table A1: Results on the full POPE dataset. Some results are cited from [19].

Dataset	Setting	Model	Decoding	Accuracy \uparrow	Precision	Recall	F1 Score \uparrow	
COCO	Random	LLaVA1.5	Regular	83.29 _(±0.35)	92.13 _(±0.54)	72.80 _(±0.57)	81.33 _(±0.41)	
			AGLA	87.46 _(±0.02)	97.52 _(±0.20)	76.87 _(±0.10)	85.97 _(±0.02)	
		InstructBLIP	Regular	80.71 _(±0.73)	81.67 _(±0.67)	79.19 _(±1.14)	80.41 _(±0.80)	
			AGLA	87.63 _(±0.19)	93.88 _(±0.26)	80.51 _(±0.31)	86.68 _(±0.21)	
		Popular	LLaVA1.5	Regular	81.88 _(±0.48)	88.93 _(±0.60)	72.80 _(±0.57)	80.06 _(±0.05)
				AGLA	86.12 _(±0.10)	94.33 _(±0.30)	76.87 _(±0.10)	84.71 _(±0.10)
	InstructBLIP		Regular	78.22 _(±0.84)	77.87 _(±1.03)	78.85 _(±0.52)	78.36 _(±0.76)	
			AGLA	84.63 _(±0.23)	87.75 _(±0.19)	80.51 _(±0.31)	83.97 _(±0.25)	
	Adversarial		LLaVA1.5	Regular	78.96 _(±0.52)	83.06 _(±0.58)	72.75 _(±0.59)	77.57 _(±0.57)
				AGLA	83.87 _(±0.10)	89.48 _(±0.20)	76.76 _(±0.20)	82.63 _(±0.10)
		InstructBLIP	Regular	75.84 _(±0.45)	74.30 _(±0.63)	79.03 _(±0.68)	76.59 _(±0.40)	
			AGLA	81.90 _(±0.15)	82.76 _(±0.09)	80.58 _(±0.31)	81.66 _(±0.18)	
VQA	Random	LLaVA1.5	Regular	83.45 _(±0.48)	87.24 _(±0.68)	78.36 _(±0.54)	82.56 _(±0.50)	
			AGLA	89.28 _(±0.27)	93.18 _(±0.14)	84.76 _(±0.45)	88.77 _(±0.30)	
		InstructBLIP	Regular	80.91 _(±0.34)	77.97 _(±0.59)	86.16 _(±0.88)	81.86 _(±0.32)	
			AGLA	87.80 _(±0.49)	86.76 _(±0.79)	89.22 _(±0.14)	87.97 _(±0.43)	
		Popular	LLaVA1.5	Regular	79.90 _(±0.33)	80.85 _(±0.31)	78.36 _(±0.54)	79.59 _(±0.37)
				AGLA	85.63 _(±0.27)	86.27 _(±0.32)	84.76 _(±0.45)	85.51 _(±0.28)
	InstructBLIP		Regular	76.19 _(±0.80)	72.16 _(±0.69)	85.28 _(±0.79)	78.17 _(±0.73)	
			AGLA	82.27 _(±0.23)	78.33 _(±0.27)	89.22 _(±0.14)	83.42 _(±0.20)	
	Adversarial		LLaVA1.5	Regular	74.04 _(±0.34)	72.08 _(±0.53)	78.49 _(±0.38)	75.15 _(±0.23)
				AGLA	78.85 _(±0.12)	75.83 _(±0.17)	84.71 _(±0.15)	80.03 _(±0.09)
		InstructBLIP	Regular	70.71 _(±0.76)	65.91 _(±0.74)	85.83 _(±0.80)	75.56 _(±0.57)	
			AGLA	74.79 _(±0.15)	69.33 _(±0.12)	88.91 _(±0.32)	77.91 _(±0.15)	
GQA	Random	LLaVA1.5	Regular	83.73 _(±0.27)	87.16 _(±0.39)	79.12 _(±0.35)	82.95 _(±0.28)	
			AGLA	88.89 _(±0.27)	92.53 _(±0.27)	84.60 _(±0.34)	88.39 _(±0.29)	
		InstructBLIP	Regular	79.65 _(±0.24)	77.14 _(±0.43)	84.29 _(±0.36)	80.56 _(±0.18)	
			AGLA	86.46 _(±0.27)	85.84 _(±0.48)	87.31 _(±0.21)	86.57 _(±0.23)	
		Popular	LLaVA1.5	Regular	78.17 _(±0.17)	77.64 _(±0.26)	79.12 _(±0.35)	78.37 _(±0.18)
				AGLA	83.67 _(±0.62)	83.05 _(±0.85)	84.60 _(±0.35)	83.82 _(±0.56)
	InstructBLIP		Regular	73.87 _(±0.58)	69.63 _(±0.54)	84.69 _(±0.68)	76.42 _(±0.52)	
			AGLA	78.67 _(±0.35)	74.44 _(±0.38)	87.31 _(±0.21)	80.36 _(±0.29)	
	Adversarial		LLaVA1.5	Regular	75.08 _(±0.33)	73.19 _(±0.49)	79.16 _(±0.35)	76.06 _(±0.24)
				AGLA	80.66 _(±0.20)	78.30 _(±0.19)	84.82 _(±0.37)	81.43 _(±0.21)
		InstructBLIP	Regular	70.56 _(±0.53)	66.12 _(±0.32)	84.33 _(±1.05)	74.12 _(±0.58)	
			AGLA	75.18 _(±0.25)	70.19 _(±0.23)	87.53 _(±0.20)	77.91 _(±0.21)	

improvement) on all LVLMS. And the improved performance on popular and adversarial (i.e., co-occurrence) settings of different subsets validates that our model can better mitigate the statistical bias of LVLMS by addressing the *attention collapse* issue, where the results are consistent with our analysis in Sec. 3.

A5 Effect of Different Decoding Strategies

In addition to the direct sampling decoding strategy discussed in the main paper, we also present an ablation study with various decoding strategies on the POPE-COCO dataset with the adversarial setting using LLaVA-1.5. The experiment includes six kinds of additional decoding strategies: Top P sampling [67] ($p = 0.7$), Top K sampling [73] ($k = 50$), Greedy decoding [74] ($\alpha = 1$ and $\beta = 0.1$), Temperature sampling [75] ($t = 0.5$), Top P sampling with temperature ($p = 0.7$ and $t = 0.5$) and Top K sampling with temperature ($k = 50$ and $t = 0.5$). The results in Table A2 indicate that AGLA consistently contributes to mitigating object hallucinations, irrespective of the decoding strategies adopted. The consistent improvement underscores the robustness and effectiveness of our model across different decoding strategies for LVLMS.

A6 Results on Perception-related MME

To validate the effectiveness of our model for enhancing general perception capability for LVLMS, we perform experiments on the perception-related tasks of the MME benchmark [71]. As shown in Table A3, our model obtains much better performance than regular baselines and achieves uniformly

Table A2: An ablation study of different decoding strategies. Regular means sampling from the original distribution.

Decoding Strategy	Model	Accuracy \uparrow	Precision	Recall	F1 Score \uparrow
Top P	Regular	80.13	84.45	73.87	78.81
	AGLA	84.23	89.84	77.20	83.04
Top K	Regular	78.50	82.07	72.93	77.23
	AGLA	83.80	89.24	76.87	82.59
Greedy	Regular	83.63	89.44	76.27	82.33
	AGLA	85.00	90.70	78.00	83.87
Temperature	Regular	81.77	86.91	74.80	80.40
	AGLA	84.33	89.92	77.33	83.15
Top P + Temperature	Regular	81.50	86.49	74.67	80.14
	AGLA	84.50	90.15	77.47	83.33
Top K + Temperature	Regular	80.60	85.20	74.07	79.24
	AGLA	84.33	89.92	77.33	83.15

Table A3: Results on MME perception-related tasks. Some results with LLaVA 1.5 are cited from [19].

Model	Decoding	Existence	Count	Position	Color	Posters	Celebrity	Scene	Landmark	Artwork	OCR	Perception Total
LLaVA1.5	Regular	175.67	124.67	114.00	151.00	127.82	113.59	148.30	129.95	102.20	92.00	1279.19
	DOLA	175.00	108.33	90.00	138.33	121.43	108.82	146.50	124.12	107.50	112.50	1232.54
	OPERA	180.67	133.33	123.33	155.00	134.69	116.76	152.75	133.01	103.25	100.00	1332.79
	VCD	184.66	138.33	128.67	153.00	132.11	120.94	152.20	140.45	109.60	104.00	1363.96
	AGLA	195.00	153.89	129.44	161.67	137.07	126.96	157.42	160.13	116.08	135.00	1472.66
InstructBLIP	Regular	161.67	62.22	63.33	114.44	120.41	94.80	143.00	131.74	96.92	80.83	1069.36
	DOLA	175.00	50.00	46.67	113.33	130.27	96.18	148.25	131.41	99.25	72.50	1062.86
	OPERA	175.00	55.00	50.00	118.15	122.86	80.00	149.25	138.79	90.75	65.00	1044.80
	VCD	170.00	61.67	57.22	114.44	121.09	104.41	140.75	140.96	103.08	82.50	1096.12
	AGLA	180.00	63.33	65.56	119.44	130.38	96.57	150.58	135.76	97.50	70.00	1109.12

improvement than previous state-of-the-art models. The improvement may come from the ensemble of local and global image attention to capture both discriminative and generative features, which is important for enhancing the visual perceptual abilities of LVLMs.

A7 Prompt for GPT-4 Aided Evaluation

To evaluate the overall quality of open-ended generation, we utilize GPT-4 to assess the accuracy and detailedness of LVLMs’ responses, following previous works [32, 19]. The prompt configurations are detailed in Table A4. Furthermore, we present an illustrative example in Fig. A1 for a better understanding of the evaluation process of GPT-4.

A8 More Qualitative Results

In order to demonstrate the quality of generated responses by different models more clearly, we present more qualitative results on the CHAIR evaluation [49] in Fig. A2 and A3. From the results, we can see that our model can generate captions with fewer object hallucinations, without loss of detailedness of the captions, which is consistent with the results in Table 2 and 3.

Table A4: The prompt for GPT-4 to evaluate captions with Accuracy and Detailedness, following previous works [32, 19].

<hr/> <p>Description: AI that scores image description accuracy and detailedness.</p> <hr/>
<p>Instructions:</p> <p>You are an AI designed to evaluate and score the performance of two AI assistants in describing a given image. Your primary focus is on the accuracy and detailedness of their descriptions. You will assess the accuracy by checking for hallucinations - any part of the description that is inconsistent with the image content. For detailedness, you will consider how rich the response is in necessary details, excluding any hallucinated parts. You will provide scores on a scale from 1 to 10 for each assistant separately, based on these criteria. After scoring, you will offer an explanation for your evaluation, ensuring it is free from bias and not influenced by the order of presentation of the responses.</p>
<p>Input format:</p> <p>[Assistant 1] {Response 1} [End of Assistant 1]</p> <p>[Assistant 2] {Response 2} [End of Assistant 2]</p>
<p>Output format:</p> <p>Accuracy: Scores of the two answers: Reason:</p> <p>Detailedness: Scores of the two answers: Reason:</p> <hr/>

[Prompt]

Please describe this image in detail.

[Image]



[Assistant 1]

The image features a large dog sitting in front of a full-length, highly detailed portrait of itself. The dog wears a bandana and appears to be the main subject of the painting. It seems to be a captivating artwork that captures the unique and intricate beauty of the dog. In the background, a person can also be seen standing slightly to the left of the dog, possibly observing or admiring the painting. The scene creates an interesting contrast between the real-life dog and its depiction in the artwork.

[End of Assistant 1]

[Assistant 2]

The image features a dog painted to resemble a human woman. The dog is wearing a dress and a scarf, giving it the appearance of a Renaissance portrait. It is positioned in front of a landscape background that includes a water body and a mountain, adding an artistic touch to the overall scene. The dog's body language suggests that it is posing for the portrait, creating a captivating visual effect.

[Assistant 2]

[GPT-4 Output]

Accuracy:

Scores of the two answers:

Assistant 1: 1

Assistant 2: 9

Reason:

Assistant 1 inaccurately describes the image, hallucinating a live dog in front of a portrait and a person in the background, none of which exist in the image. This significant misrepresentation results in a very low accuracy score.

Assistant 2 accurately identifies that the image is of a dog painted in the style of a human Renaissance portrait, correctly noting the attire and setting, aligning well with the content of the image.

Detailedness:

Scores of the two answers:

Assistant 1: 2

Assistant 2: 8

Reason:

Assistant 1 provides detail in describing elements that do not exist in the image, such as a live dog, a bandana, and a background person. The non-existent details are irrelevant to the actual image content, thereby reducing the score for detailedness despite the descriptive attempt.

Assistant 2 offers a more detailed description of the actual image, noting the dog's dress and scarf in a Renaissance style and the landscape background. The details about the dog's body language and the scene add to the richness of the description, enhancing its detailedness score.

[End of GPT-4 Output]

Figure A1: An example of the GPT-4 evaluation in open-ended generation tasks. “Assistant 1” is Regular decoding and “Assistant 2” is the proposed model AGLA.

[Prompt]

Please describe this image in detail.

[Regular]

The image features a unique, colorful display of numerous umbrellas hanging from the ceiling of a building, likely a store or a public space. The umbrellas are in various shapes and sizes, creating a vibrant and eye-catching scene. Apart from the umbrellas, there are also several **balls** scattered throughout the display, adding more color and visual interest to the scene. The **balls** are of different shapes and sizes, further enhancing the overall aesthetic. The umbrellas are suspended at different heights, with some closer to the bottom and others higher up.

This artistic arrangement gives the impression of a festive or whimsical atmosphere, attracting attention and making it a memorable experience for visitors.

[VCD]

The image presents a sky full of various luminous umbrellas suspended under a glass roof, creating a colorful atmosphere. There are different sizes and colors of umbrellas, adding to the vibrant, whimsical display. Beneath the umbrellas, the shopping floor exudes a luminous interior design. There are a few **people** scattered around the scene, possibly passersby or visitors to the shop beneath the roof. The brightly colored umbrellas and glass roof adorn the interior of the mall, giving it an artistic and captivating vibe.

[OPERA]

The image features a large indoor space filled with numerous colorful umbrellas suspended from the ceiling. These umbrellas come in various sizes and colors, creating a vibrant and eye-catching display. The umbrellas are spread throughout the room, with some closer to the foreground and others further in the background. In addition to the umbrellas, there are several chairs scattered around the room, some **people** sit and enjoy the unique atmosphere created by the umbrellas. The combination of the umbrellas and chairs creates a visually appealing and inviting environment.

[DOLA]

The image showcases a large and colorful installation of umbrellas suspended from the ceiling of a building, creating an artistic and vibrant atmosphere. The umbrellas are of various sizes and colors, adding a lively touch to the scene. In total, there are **10 umbrellas** visible in the image, with some placed higher and others hanging lower. A few chairs can also be seen scattered throughout the scene, possibly serving as a part of the installation or simply placed for decoration. These chairs are positioned at different heights and angles, adding more visual interest to the overall display.

[AGLA]

The image features a large indoor space with a unique and colorful installation of numerous umbrellas hanging from the ceiling. The umbrellas are of various sizes and colors, creating an eye-catching display. Some umbrellas are red, and they are all suspended from the ceiling at different heights. In addition to the umbrellas, there are several chairs scattered throughout the space, adding to the overall aesthetic. The chairs are positioned at different angles and heights, contributing to the dynamic and visually interesting atmosphere of the room.

[Image]



Figure A2: An example of generated captions by different decoding methods. Hallucinated content is marked in **red**.

[Prompt]

Please describe this image in detail.

[Image]



[Regular]

The image showcases a family gathered around a dining table outside, enjoying a meal together. There are multiple chairs placed around the table, and several family members can be seen sitting or standing in the background as well. The table is adorned with a mix of dishes and cutlery, such as wine glasses, cups,

forks, and *knives*. Several *bottles* are also scattered around the table, suggesting different beverages being served. The scene is set in an outdoor area, possibly in a park or similar environment, adding to the family's enjoyment of their time together.

[VCD]

The scene features a crowded restaurant patio area lined with several dining tables, each with chairs arranged around them. Two poofy chairs are prominently visible placing a family, consisting of a father, two young children, and a grand lady, at one of the tables. They seem to be enjoying a meal with utensils like *forks*, *knives*, and cups laid out. In the vicinity, there's an array of other people eating, conversing or engaged in other daily activities. Some can be seen near other dining tables, while others are sitting or standing around the area. The restaurant itself has a few *potted plants* inside as well as a collection of wine glasses, giving an impression of a lively and pleasant atmosphere.

[OPERA]

The image depicts a group of people, including a man, a woman, and two children, sitting around a dining table outfitted with a red and white checkered tablecloth. They are enjoying a meal together, with plates of food and wine *bottles* placed on the table. There are several chairs surrounding the table, and a few more people can be seen in the background, likely engaged in conversation or waiting for their turn to join the meal. The dining area is furnished with additional chairs and dining tables, creating a cozy and inviting atmosphere for the family gathering.

[DOLA]

The image depicts a lively outdoor restaurant setting with several people dining together at picnic tables. A man, a woman, and two children are seated at a dining table, sharing a meal together. The table is set with various items such as *forks*, *spoons*, *knives*, and wine glasses. There are also cups, bowls, and a couple of *bottles* placed on the table. The dining area is surrounded by numerous chairs, and there are additional tables and benches spread throughout the scene. The restaurant is bustling with activity, and people can be seen at different locations, either sitting at tables or walking around. Overall, it's a warm and inviting atmosphere, showcasing a family enjoying a meal in a relaxed and convivial setting.

[AGLA]

The image features a family sitting around a dining table in an outdoor restaurant. They are enjoying a meal together, with various plates of food, cups, and wine glasses spread across the table. There are multiple chairs surrounding the table, with some placed close to the family and others further away. A few other people can be seen in the background, likely other diners at the restaurant. The atmosphere appears to be casual and pleasant, as the family enjoys their time together.

Figure A3: An example of generated captions by different decoding methods. Hallucinated content is marked in *red*.